Auger electron emission from Si(111) surface during 11 keV Ar^+ ion sputtering

K. Kawai, Y. Sakuma, M. Kato and K. Soda

Department of Quantum Engineering, Graduate School of Engineering, Nagoya University,

Furo-cho, Chikusa-ku, Nagoya 464-8603, Japan

Ion sputtering experiments were carried out for a Si(111)-7×7 surface, irradiated by 11 keV Ar^+ continuous beam. The energy spectra of ejected secondary electrons were measured by cylindrical mirror analyzer (CMA). The dependence of the Auger electron spectrum on the ion incidence angle θ, measured from the surface normal, was investigated by varying θ from 0° to 80°. The Auger electron yield increases with increasing of the incidence angle of primary ion. This angular dependence is similar to that of sputtering yield of Si and could be reasonably understood in terms of ion range, escape depth for electron and sputtering ion.

1. Introduction

The ion sputtering is used as various technical applications and also as analytical tools, e.g., second ion mass spectrometry (SIMS). SIMS is useful for compositional analysis of material surfaces. However, it is important to clarify the ionization mechanism of sputtered species for the quantitative analysis. In the case of Si sputtered by Ar^+, Si^{2+} is produced at high efficiency even for a well-cleaned surface [1]. Several processes for the Si^{2+} production are suggested [2, 3]. We have paid an attention to the production mechanism of Si^{2+} ions during ion sputtering and have realized the importance of Si^{0*} or Si^{+*} as precursors of the Si^{2+} ion [3]. There would be many possible ionization processes for Si^{2+} ion. Among them, the likely processes are shown in Fig.1, where the ionization followed by Auger electron emission during sputtering are schematically described. The promotion of Si 2p electron occurs on an energetic collision (>1 keV) of Si-Si inside a Si solid, and 2p hole is created. The Auger electrons released in the vacuum and in the solid are referred to as Atomic Auger and Bulk Auger electrons, respectively.

In order to investigate detailed mechanism, we have planned the coincident measurement of sputtered-ion and Auger-electron, which may distinguish the individual processes of ionization. As the first step for this plan, we measured the energy spectra of

the ion induced Auger electron for various incidence angles of 11 keV Ar^+ beam, and we observed an interesting correlation between Atomic and Bulk Auger electron yields. In this paper, we report the observed correlation and provide its interpretation.

2. Experiment

The experimental setup consisted of an ion source, a sample manipulator with a heater, a cylindrical mirror analyzer (CMA) with an energy resolution of $E/\Delta E$=50, a low energy electron diffraction (LEED) apparatus and a measuring system. Base pressure of the main scattering chamber was 5×10^{-11} Torr. Since the axis of CMA was fixed at an angle of 45° with respect to the primary beam direction, only the incidence angle of ion to the sample surface could be changed by rotating the sample.

The sample was n-type Si(111) wafer of 3 Ωcm in resistivity and 5 mm ×10 mm in size. As the initial surface of the sample was covered with oxygen and other impurities, a clean Si surface was prepared by several repetitive cycles of 11 keV Ar^+ sputtering and annealing at ~1200 K. Then, residual impurities reduced below the detection limit of AES, and LEED image showed 7×7 pattern.

All measurements of secondary electrons were performed on such a Si(111)-7×7 surface by using 11 keV Ar^+ continuous beam as a primary ion beam. The secondary

electrons ejected at the angle of 45°, with respect to the direction of primary beam, were energy-analyzed by the CMA. The dependence of the secondary electron yield on the incidence angle of primary ion was investigated by varying the incidence angle θ from 0°, 30°, 45°, 60°, 70°, 75° to 80°, where θ is measured from the surface normal.

3. Results and Discussion

The Si Auger electron spectrum measured at the incidence angle of 45° is shown in Fig.2, where the electron intensity has been normalized by the fluence of incident ion. As is seen in the figure, the spectrum exhibits a broad structure with local peaks and shoulders. Arrows A ~ E in Fig.2 indicate the energy positions of the Auger electron released by individual Auger transitions. The electron configurations corresponding to Auger transitions and the energies of A ~ E are summarized in Table 1 [4, 5]. The A ~ D can be assigned to the Si LMM Auger process of the atom/ion sputtered into the vacuum. These Auger electrons are the Atomic Auger electrons, named earlier. In addition to the Atomic Auger electrons, there is a contribution from the Auger decay of excited Si inside the sample, i.e., the Bulk Auger electrons, which exhibits a broad spectrum structure. Unlike the Atomic Auger electrons, the Bulk Auger electrons do not show a sharp peak structure, because it corresponds to the LVV Auger transition and is

broadened due to the width of valence band. The arrow E indicates the highest energy position of the Bulk Auger electrons. Thus, the observed spectrum is the discrete peaks of the Atomic Auger electrons superposed on the broad Bulk Auger contribution [4]. A small peak marked by 'X' in a Fig.2 is always observed in different experimental conditions, although its physical origin is unidentified.

The measured Auger electron spectra for various incidence angles ($\theta = 0° \sim 80°$) are shown in Fig.3. The angle dependence of the Atomic Auger yield of 70 ~ 80 eV (spectrum part windowed in Fig.3) is shown in Fig.4(a). The intensity of Atomic Auger was estimated by subtracting the Bulk Auger contribution from the observed spectrum. The energy range of 70 ~ 80 eV corresponds to the Atomic Auger transition of Si^{+*} $2p^5 3s^2 3p^2 \rightarrow 2p^6 3s3p$ (Table 1). Figure 4(b) shows the Bulk Auger intensity of 93 ~ 96 eV (windowed in Fig.3), in which the Atomic Auger does not contribute. Both Atomic and Bulk Auger yields increase with increasing the incidence angle until ~75°, and then decrease. However, the peak around $\theta = 75°$ of the Bulk Auger yield increases and decreases more steeply than the Atomic Auger yield.

To study the correlation between the sputtering process and Auger yield, we calculated the Si sputtering yield and the Ar ion range, *etc*., for the various incidence angles by using Computer Code SRIM [5]. The calculated angular dependence of Si

sputtering yield is also shown in Fig. 4.

As is shown in Fig.4, the angle dependence of both the Atomic and Bulk Auger yields qualitatively resemble that of calculated sputtering yield. The Atomic Auger yield slightly better resembles the calculated sputtering yield than the Bulk one. This fact appears natural, as the Atomic Auger electrons are ejected from the excited ion Si^{+*} sputtered into the vacuum. Here, we note that the simulations did not distinguish the charge states and excited states of the atom/ion and, moreover, the surface conditions were different between SRIM and the experiments. The sample assumed in SRIM simulations is amorphous, and the surface is not eroded by incident ions, that is, the sample is reset after each ion shot to the sample. In contrast, the sample in the experiments was a single crystal and its surface was continuously eroded by Ar^{+} bombardment.

A schematic model of the Auger electron emission is shown in Fig.5. According to the SRIM simulations, the accumulation of collision cascades after 100,000 ion shots becomes spherical. This spherical collision cascades is referred to as the collision cascade region. The atomic collisions and the electronic excitations of Si intensively take place in the collision cascade region. For larger incidence angles but less than θ =75°, the collision cascade region is inclined toward the surface and it more spreads out

at the surface. This leads to that: the sputtering yield increases and the number of excited Si near the surface increases, and accordingly, both the Atomic and Bulk Auger yields increase. For the incidence angles larger than 75°, the surface reflection of the primary Ar^+ significantly occurs and the collision cascade region is not well developed, and, in fact, at the limit of 90°, all primary ions would be reflected. Therefore, both Atomic and Bulk Auger yields decrease.

The above qualitative model may be discussed in terms of the escape depth. The Bulk Auger yield may be explained in terms of the escape depth λ_e of Si LVV Auger electron (~95 eV); for the Auger electron emitted at the depth *z*, the probability of escape from the surface is given by $\exp(-z/\lambda_e)$. Similarly, we introduce the effective escape depth for the sputtered Si^{+*}. The sputtering occurs by Ar-Si direct collision and the propagation of Si-Si chain collision to the surface, which we deal with by using the effective sputtering depth, denoted by λ_{Si}.

As is mentioned earlier, the peak around 75° of the Bulk Auger yield increases and decreases more steeply than the Atomic Auger yield. If we assume that the fraction of Si^{+*} $2p^5 3s^2 3p^2$ ion does not depend on the incidence angle of Ar^+, this observation suggests that λ_{Si} is slightly longer than λ_e (λ_e <1 nm) [7].

Since the ion range of 11 keV Ar in a solid Si is about 15 nm, λ_e and λ_{Si} are

significantly shorter than the ion range. Therefore, for incidence angles close to the surface normal incidence, both the Atomic and Bulk Auger yields are negligibly small (Fig.4).

4. Conclusion

The Auger electron yield shows a significant dependence on the incidence angle θ of the primary ion beam. For larger incidence angles, the collision cascade region is well developed near the surface. Then, the sputtering yield and the number of excited Si^{*} near the surface are increased, as verified by SRIM. Therefore, both the Atomic and Bulk Auger electron yields are also increased. From a different angular dependence of Atomic and Bulk Auger electron yield, the effective sputtering depth of Si^{+*} $2p^{5}3s^{2}3p^{2}$ is slightly longer than the escape depth of Si LVV Auger electron.

References

[1] N. Shinde, K. Morita, S. D. Dhole, and D. Ishikawa, Nucl. Instrum. Meth. B **182** (2001) 135.

[2] K. Wittmaack, Nucl. Instr. And Methods. **170** (1980) 565.

[3] Y. Sakuma, M. Kato, N. Shinde, S. Yagi, and K. Soda, Appl. Surf. Sci. **255** (2008) 908.

[4] R. Whaley and E. W. Thomas, J. Appl. Phys. **56** (1984) 1505.

[5] S.V. Pepper, Phys. Rev. Lett. 169 (1986) 14.

[6] J. F. Ziegler, Computer Code SRIM-2012, http://www.srim.org/.

[7] R. Shimizu, Jpn. J. Appl. Phys. Rev. A 29 (1984) 116.

Table 1

Table 1. Possible transitions and the energies of the Si Auger electrons.

	Auger Transition	Energy
A	$Si^{+*}\ 2p^5 3s^2 3p^2 \rightarrow 2p^6 3s^2$	67 eV
B	$\rightarrow 2p^6 3s3p$	75 eV
C	$Si^{0*}\ 2p^5 3s^2 3p^3 \rightarrow 2p^6 3s3p^2(^2S)$	83 eV
D	$\rightarrow 2p^6 3s3p^2(^2D)$	86 eV
E	LVV Bulk Auger	95 eV

Figure Captions:

Fig.1. A schmatic of the production process of sputtered ions and Auger electrons.

Fig.2. Si Auger spectrum at incidence ion angle $\theta = 45$ °.

Fig.3. Si Auger spectra for different incidence angles. The spectra have been normalized by the fluence of incident ion. Spectra for the incidence angles of 0 ~ 45 ° are not shown, because the Auger electron yield was very small.

Fig.4. Comparison of incidence angle dependence between Auger yield and sputtering yield. Sputtering yield calculated is shown by a dotted line, and (a) Atomic Auger yield and (b) Bulk Auger yield are shown by a solid line.

Fig.5. Schematic model of Auger electron emission. The spheres are the collision cascade region. As the incidence angle increases from the surface normal, the collision cascade region is inclined toward the surface, and both the Atomic and Bulk Auger yield increase.

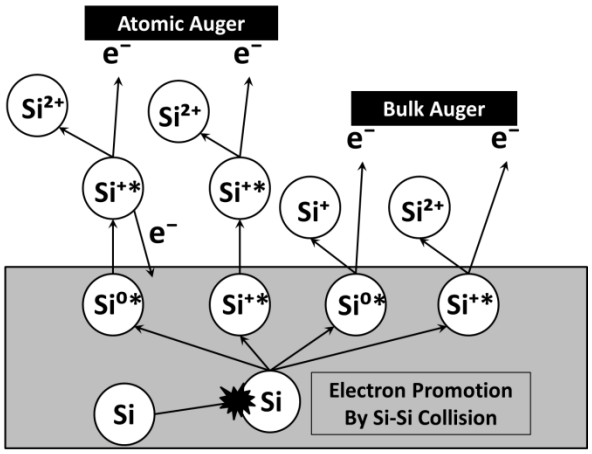
Atomic Auger
e⁻
e⁻
Si²⁺
Si²⁺
Bulk Auger
e⁻
e⁻
Si⁺*
Si⁺*
Si⁺
Si²⁺
e⁻
Si⁰*
Si⁺*
Si⁰*
Si⁺*
Si
Si
Electron Promotion
By Si-Si Collision

Fig. 1

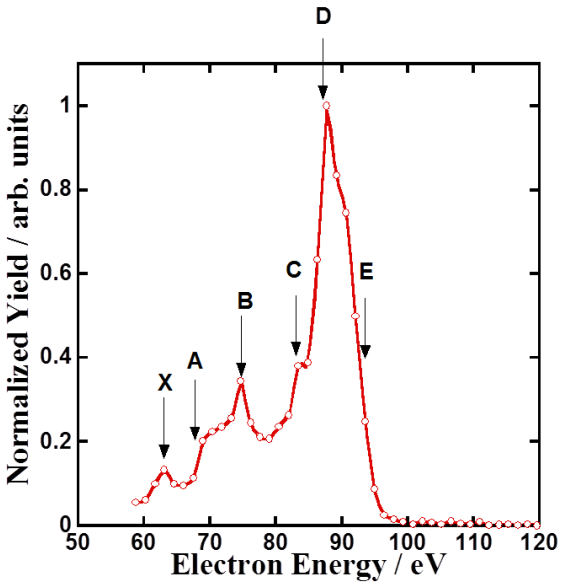
D
C
E
B
A
X
Normalized Yield / arb. units
Electron Energy / eV
0
0.2
0.4
0.6
0.8
1
50
60
70
80
90
100
110
120

Fig. 2

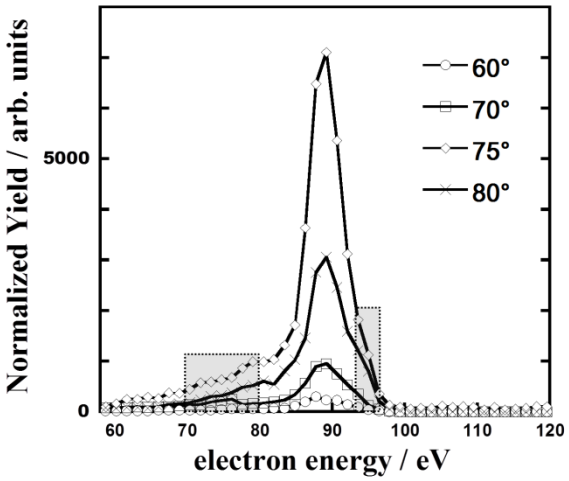
Normalized Yield / arb. units
5000
0
60
70
80
90
100
110
120
electron energy / eV
60°
70°
75°
80°

Fig.3

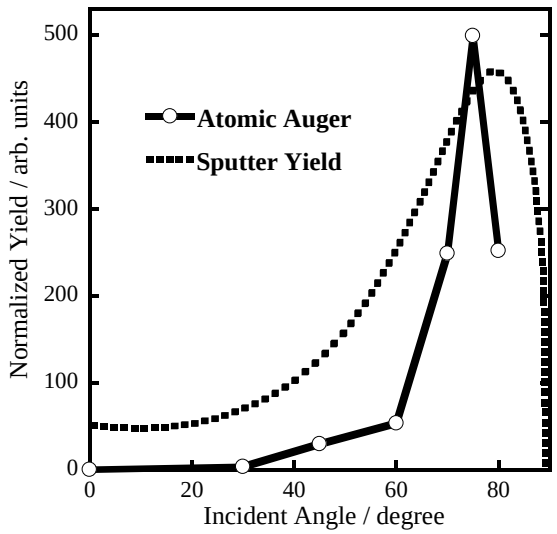

Fig. 4(a)

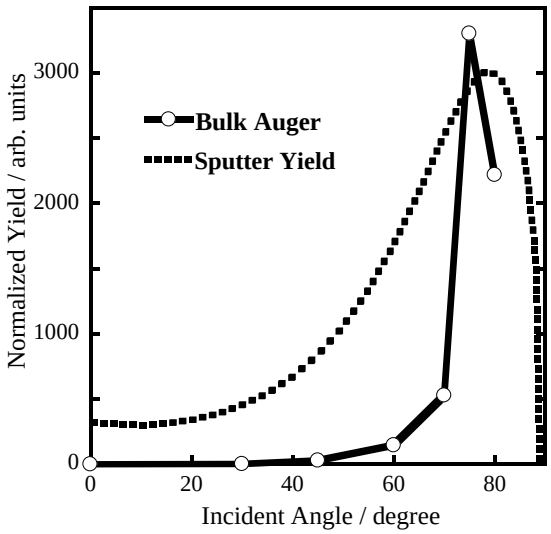

Fig. 4(b)

2-column requested.

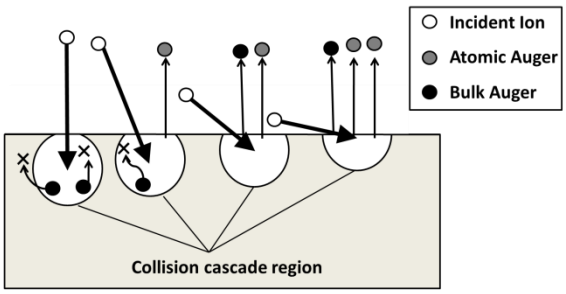
Incident Ion
Atomic Auger
Bulk Auger
Collision cascade region
Fig.5